CORBASS

CORrelation BAsed SnapShot models of the archeomagnetic field

D1266 | EGU2020-6808

Maximilian Arthus Schanner[*,1], Stefan Mauerberger[2], Monika Korte[1] and Matthias Holschneider[2]

*: arthus@gfz-potsdam.de
1: GFZ German Research Centre for Geosciences, Potsdam, Germany
2: Institute of Mathematics, University of Potsdam, Germany

EGU 2020 - Sharing Geoscience Online

There is a supplementary audio file available for this display, containing some more details about the presented work.

You can find it here:

`ftp://ftp.gfz-potsdam.de/home/mag/arthus/EGU2020_D1266_Supplementary.mp3`

Motivation

Global reconstructions of geomagnetic core field for the past millennia are useful to investigate the geodynamo process or estimate geomagnetic shielding against galactic cosmic rays and they find application in archeo- and paleomagnetic dating. Reconstructions are typically built from volcanic and archeomagnetic samples providing records of the ancient Earth's magnetic field. Unfortunately, on a global scale records are clustered, unevenly distributed towards the Western Eurasian region and corrupted by measurement uncertainties. This considerably complicates the reconstruction of the ancient Earth's magnetic field. So far, the resulting uncertainties related to modeling, in particular due to the uneven data distribution, have never been quantified well.

In this display, we present a new concept to model snapshots of the global archeomagnetic field. We adress the problem of uneven data distribution, as well as the non-linear relation between archeomagnetic records and the field itself, by pursuing a fully Bayesian approach. To demonstrate the potential of this approach, we present results from a case study at the end of this display.

Data distribution

We use archeomagnetic data (declination, inclination, intensity) in the interval [800, today] with ≈8000 records in total, taken from GEOMAGIA[1]. The figure below shows the temporal distribution of the number of records, the next slide shows the spatial distribution. Strong variations in number of data are partly due to accuracy or rounding of age information.

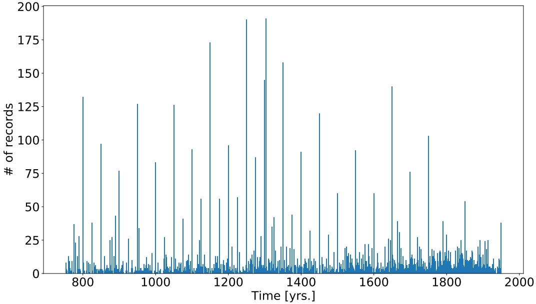

[1] Brown et al. 2015.

Data distribution

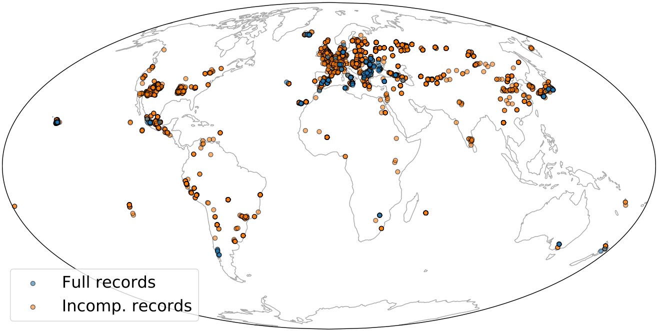

The blue dots refer to complete records, where declination, inclination and intensity are reported, the orange dots refer to records where at least one component is missing. Note, that these are all data locations, and the data distribution varies with time.

Data distribution

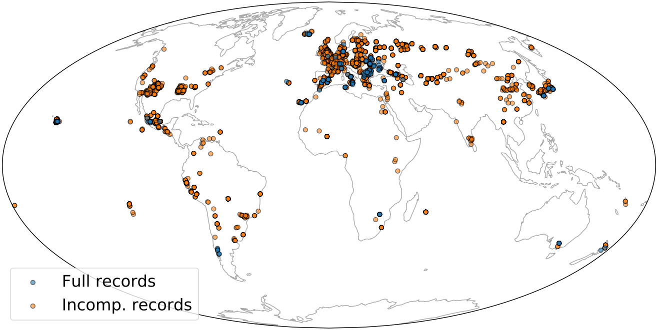

Both distributions are highly uneven. Here, we focus on the spatial distribution, as we present snapshot models. Temporal evolution, and thus tackling the uneven distribution in time, is the aim of future work.

Further challenges

Archeomagnetic modeling poses two other challenges we are going to adress. First, the observations are non-linearly related to the modeled vector field components. Second, uncertainties arising not only from the uneven distribution in space, but also from the measurement process and from the modeling process have to be incorporated.

Modeling strategy

Almost all existing models are based on truncated spherical harmonics[2].

Instead, we use Gaussian processes[3] to address the problem of uneven data distribution. The Gaussian process posterior distribution is characterized by a mean- and a covariance function, which are calculated using

$$\begin{aligned} \mathbb{E}[\boldsymbol{B}(\boldsymbol{x})|o] &= \bar{\boldsymbol{B}}(\boldsymbol{x}) + \Sigma_{\boldsymbol{B}O}\Sigma_O^{-1}\left(o - \bar{O}\right) \\ \mathrm{Cov}[\boldsymbol{B}(\boldsymbol{x}), \boldsymbol{B}(\boldsymbol{y})|o] &= K_{\boldsymbol{B}}(\boldsymbol{x}, \boldsymbol{y}) - \Sigma_{\boldsymbol{B}O}\Sigma_O^{-1}\Sigma_{\boldsymbol{B}O}^\top , \end{aligned} \tag{1}$$

where the Σ-matrices are built from a correlation kernel $K_{\boldsymbol{B}}$

$$\begin{aligned} \Sigma_O &= \mathrm{Cov}[O, O] = \{K_{\boldsymbol{B}}(\boldsymbol{z}_i, \boldsymbol{z}_j)\}_{i,j=1,\dots,n} \\ \Sigma_{\boldsymbol{B}O} &= \mathrm{Cov}[\boldsymbol{B}(\boldsymbol{x}), O] = \{K_{\boldsymbol{B}}(\boldsymbol{x}, \boldsymbol{z}_i)\}_{i=1,\dots,n} \ . \end{aligned}$$

---

[2] Gubbins et al. 1985.

[3] Rasmussen et al. 2006.

Kernel construction

The correlation kernel is constructed following Holschneider et al. (2016). The correlation kernel for the magnetic potential reads

$$K_\Phi(\boldsymbol{x}, \boldsymbol{y}) = \frac{R^2}{\sqrt{1 - 2t + a^2}} \tag{2}$$

where R is a reference radius, $t = \boldsymbol{x} \cdot \boldsymbol{y}/R^2$ and $a = |\boldsymbol{x}||\boldsymbol{y}|/R^2$. The closed form (2) is called *Legendre kernel*.

The field correlations are then given by derivatives of the kernel for the potential (2). We modify the kernel in two ways. First, we seperate the dipole part from the higher orders, as we expect the field to be dipole dominated. Second, we add two parameters ϵ and ρ. ϵ is a scaling factor for the measurement errors, which we add since we believe that they may be underestimated. ρ is a factor controlling the residual level, in which contributions to the field which we do not model (e.g. the crustal field) are absorbed. The actual kernel reads

$$K_{\boldsymbol{B}} = K_{\boldsymbol{B},\mathrm{DP}}(\bar{g}_1^m, \bar{\Sigma}_1) + \lambda K_{\boldsymbol{B},\mathrm{ND}}(R) + \epsilon E + \rho P \ . \tag{3}$$

The figure below depicts the correlation structure of the non-dipole part in (3). The units are arbitrary, dark red refers to a high correlation, white to no correlation and blue to anti-correlation.

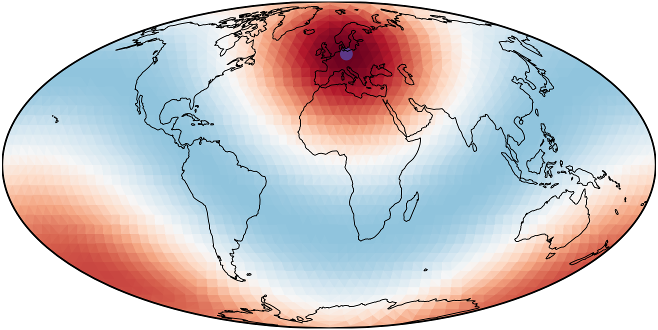

To incorporate the modeling related uncertainties, we address the model parameters in (3):

$$K_{\boldsymbol{B}} = K_{\boldsymbol{B},\mathrm{DP}}(\bar{g}_1^m, \bar{\Sigma}_1) + \lambda K_{\boldsymbol{B},\mathrm{ND}}(R) + \epsilon E + \rho P \ . \tag{3}$$

The parameters are $\bar{g}_1^m, \bar{\Sigma}_1, \lambda, R, \epsilon$ and ρ.
$\bar{g}_1^m, \bar{\Sigma}_1$, the prior dipole coefficients and covariance, are eliminated by choosing a non-informative prior for the dipole part. The reference radius basically controls the slope of the spectrum, and is estimated by comparing the prior spectrum to the IGRF models from 1900 to 2015, which is shown on the next slide.
The remaining parameters, the non-dipole variance λ, ϵ and ρ are marginalized using numerical integration.

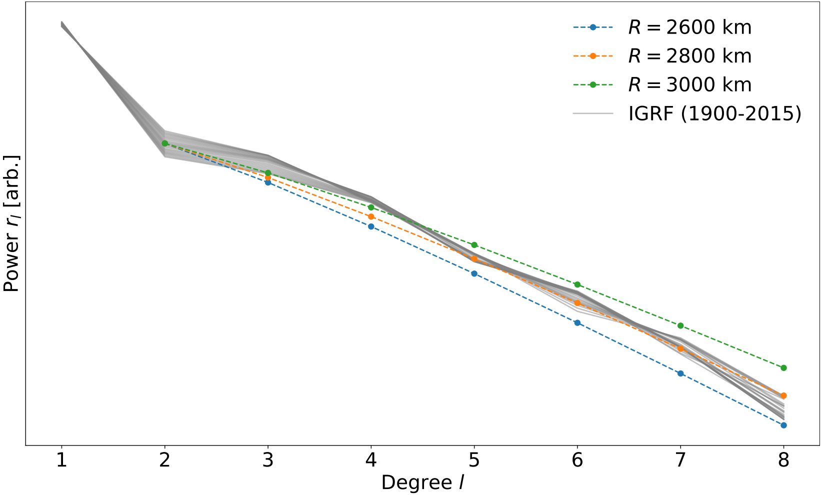
$R = 2600$ km
$R = 2800$ km
$R = 3000$ km
IGRF (1900-2015)
Power r_l [arb.]
1
2
3
4
5
6
7
8
Degree l

Finally, we use a linearization to address the problem of non-linear relations between observations and modeled quantities. However, the question arises around which model this linearization is performed. The prior model is not suited, so instead we implement a two step strategy. In a first step, the complete records are used to perform the linearization in a Laplace approximation setting. This way, a model is constructed which is then used to perform the linearization for the incomplete records in a second step.

The whole algorithm is available as a python software package, called CORBASS[4]. CORBASS makes use of the FieldTools library[5] and is available at `http://doi.org/10.5880/GFZ.2.3.2019.008`

[4]Schanner et al. 2019.

[5]Matuschek et al. 2019.

Case study

We conclude by presenting results from a case study. To conduct this study, we grouped the data into bins of 100 yrs. width. The reason for this is that we need at least 30 full records to perform the first step in the linearization strategy. The grouped data distribution is shown below, the bin we focus on in this presentation is highlighted.

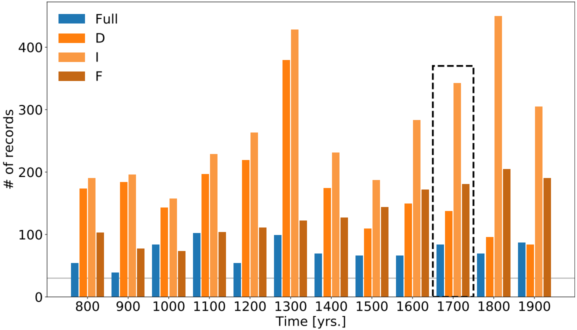

We start by showing the mean and the standard deviation of the posterior distribution for the down component Z of the magnetic field and the field's intensity F at the Earth's surface. The records are shown as orange dots. Note two things: First, one can see a high standard deviation in regions of low data coverage, while in regions covered well by data, for example in Europe, the standard deviation is low. Second, due to the strong correlation in the data, we see the South Atlantic Anomaly offshore to the west of Africa, even though there is not a single record at the anomalies position.

Field at the Earth's surface - 1700 epoch

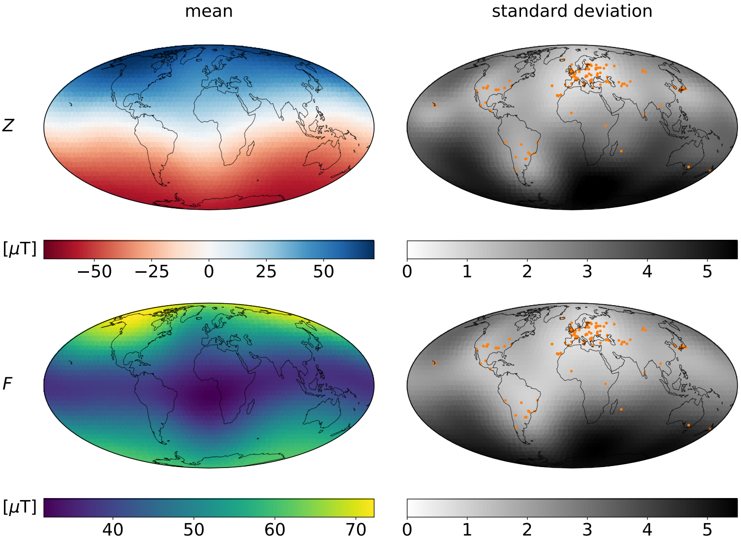

To the right, we show the posterior distribution for axial magnetic dipole g_1^0, together with comparison models[6]. The mean agrees with models using a similar database and the distribution resembles the histogram created from the ensembles provided by COV-ARCH. The mean deviates from Arhimag, which is not surprising since the latter incorporates historical records, additionally to the data we use.

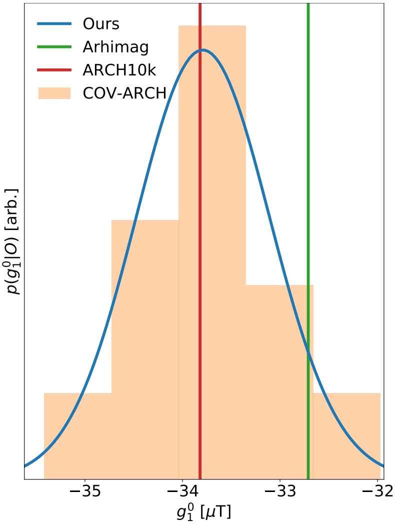

[6] Senftleben 2019; Constable et al. 2016; Hellio et al. 2018

The figure below shows the Gauss coefficient power spectrum. Our model agrees with COV-ARCH within the error bonds. Arhimag and ARCH10k report less power at degree 3 and fall off faster at higher degrees. The latter is likely due to the regularization structure underlying these models.

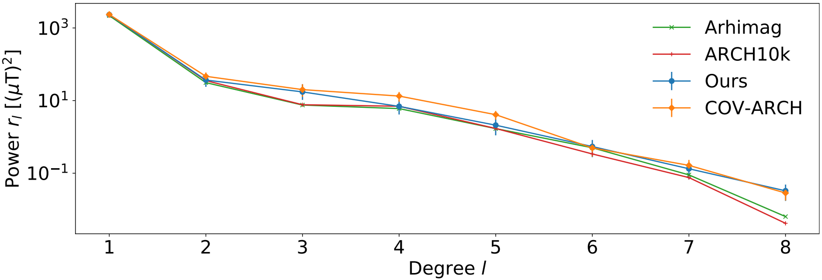

We indicate the a priori slope of our model in grey. As can be seen, from degree 5 on, our model only reproduces the slope, indicating that the data only allow reconstructions for the lower degrees.

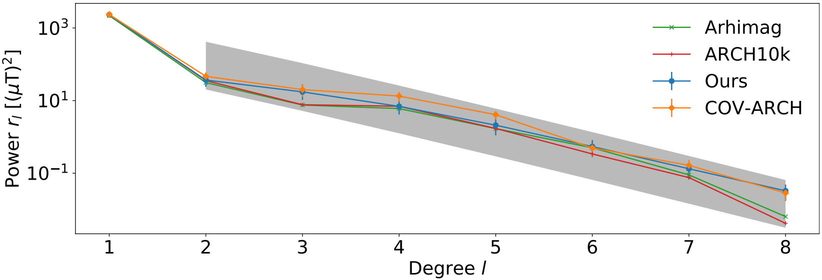

Finally, by constructing models for all bins in the database, we build a discrete time series and show the evolution for the dipole intensity. Overall the evolution agrees with the comparison models. The strong deviations at epochs 1100 and 1500 may be caused by outliers, which we haven't tested for yet.

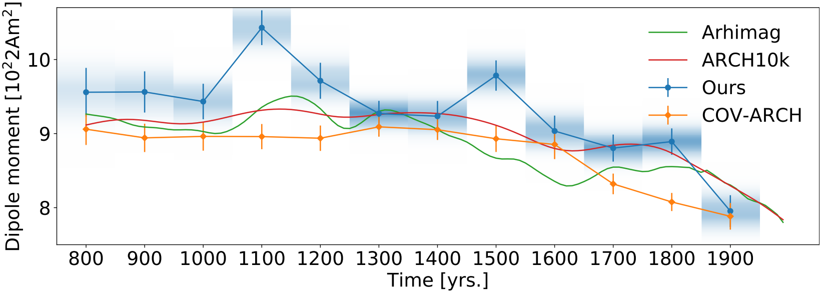

Similarly, we present the dipole axis wander (the outer circle is at a latitude of ≈40°). Again, the evolution agrees with the comparison models. Deviations for the 800 and 1100 epochs may again be caused by outliers.

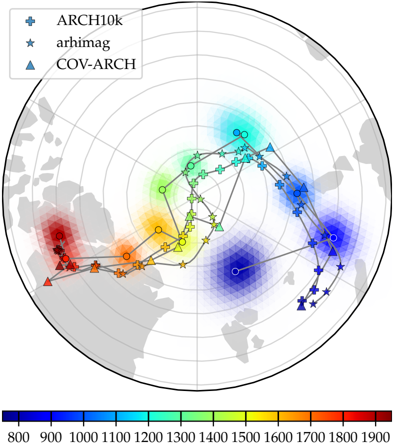

Conclusion

- We presented an algorithm to tackle the challenges posed by archeomagnetic data

Uneven data distribution	$\leftrightarrow$	Gaussian processes
Non-linear relation	$\leftrightarrow$	Two step linearization
Modeling uncertainties	$\leftrightarrow$	Marginalization of parameters

- Further, snapshot models for selected epochs were shown
- Overall, the results agree with established models

All results converged into a publication submitted to GJI[7].

[7] Mauerberger et al. submitted.

Outlook

There are several ideas how to continue this work:

- A moving window may be used to refine the time series presented above
- A temporal correlation kernel allows to tackle the uneven distribution in time
- This further allows the incorporation of the sometimes very large temporal uncertainties
- Once a time-dynamic model is available, sediment core data may be included
- The database may be increased to construct longer time series

Thank you!

References I

Brown, Maxwell C. et al. (May 2015). "GEOMAGIA50.v3: 2. A new paleomagnetic database for lake and marine sediments". In: *Earth, Planets and Space* 67.1, p. 70. ISSN: 1880-5981. DOI: 10.1186/s40623-015-0233-z. URL: https://doi.org/10.1186/s40623-015-0233-z.

Constable, Catherine, Monika Korte, and Sanja Panovska (2016). "Persistent high paleosecular variation activity in southern hemisphere for at least 10 000 years". In: *Earth and Planetary Science Letters* 453, pp. 78–86. ISSN: 0012-821X. DOI: 10.1016/j.epsl.2016.08.015.

References II

- Gubbins, D. and J. Bloxham (1985). "Geomagnetic field analysis – III. Magnetic fields on the core-mantle boundary". In: *Geophysical Journal of the Royal Astronomical Society* 80.3, pp. 695–713. ISSN: 1365-246X. DOI: 10.1111/j.1365-246X.1985.tb05119.x.
- Hellio, G. and N. Gillet (2018). "Time-correlation-based regression of the geomagnetic field from archeological and sediment records". In: *Geophysical Journal International* 214.3, pp. 1585–1607. DOI: 10.1093/gji/ggy214.
- Holschneider, M. et al. (2016). "Correlation-based modeling and separation of geomagnetic field components". In: *Journal of Geophysical Research: Solid Earth* 121.5, pp. 3142–3160. ISSN: 2169-9356. DOI: 10.1002/2015JB012629.

References III

Matuschek, Hannes and Stefan Mauerberger (2019). *Toolbox for manipulating vector fields on the sphere*. DOI: 10.5880/fidgeo.2019.033. URL: http://doi.org/10.5880/fidgeo.2019.033.

Mauerberger, Stefan et al. (submitted). *Correlation based snapshot models of the archeomagnetic field*.

Rasmussen, C.E. and C.K.I. Williams (2006). *Gaussian Processes for Machine Learning*. MIT Press, Cambridge, MA. ISBN: 026218253X.

Schanner, Maximilian and Stefan Mauerberger (2019). *CORBASS: CORrelation Based Archeomagnetic SnapShot model V.1.0*. DOI: 10.5880/GFZ.2.3.2019.008. URL: http://doi.org/10.5880/GFZ.2.3.2019.008.

Senftleben, Robin (2019). "Earth's magnetic field over the last 1 000 years". PhD thesis. University of Potsdam.

Thank you!